XII International Conference on Computational Plasticity. Fundamentals and Applications
COMPLAS XII
E. Oñate, D.R.J. Owen, D. Peric and B. Suárez (Eds)

DIRECT METHOD-BASED STATISTICAL LIMIT ANALYSIS OF WC-CO COMPOSITES

GENG CHEN, ABDELKADER HACHEMI AND DIETER WEICHERT

Institute of General Mechanics
RWTH Aachen University
Templergraben 64, 52056 Aachen, Germany
e-mail: geng@iam.rwth-aachen.de

Key words: Direct method, Limit analysis, Ultimate strength, Yield strength, Composites, Homogenization.

Abstract. In this paper, a direct method-based prediction of load-bearing capacity of non-periodic WC-Co composites is presented. The main goal is to generalize the methodology of limit analysis on periodic heterogeneous media to materials with random microstructures. For such materials, the admissible macroscopic loading domains demonstrate remarkable scatter among RVE models of identical size and constituents but different morphologies. Limit analysis is performed on samples of a group of RVE models converted automatically from scanning electron microscopy (SEM) images. The corresponding admissible loading domains are numerically determined and statistically interpreted. The obtained results for plastic limit loads by direct method are compared with those from conventional incremental analysis.

1 INTRODUCTION

In recent decades, the increasing use of particulate reinforced metal-matrix composites (PRMMC) in industry enhances the need of capable computational methods for predicting the global behavior of materials. In this study in particular global yield strength and ultimate strength reflecting the load-bearing capability of the material as important technical properties are investigated. How to determine these parameters with taking into account for the characteristics of material's microstructure is a critical issue for material research.

In PRMMCs granular shaped brittle grains are imbedded in a ductile metal-matrix [1]. The resulting geometrical complexity of the material makes modeling of representative volume elements (RVE) rather difficult. Most existing modeling techniques are restricted to 2D and can be coarsely divided into two groups: the first group consists of methods aiming to develop idealized microstructures representing major features of the original composite, while the second group of methods directly duplicate the real microstructure [2]. Due to the extensive efforts for models generation, 3D models are studied only recently and cost exceptional effort [3]. Besides the complex microstructure, the random nature of the material further increases the difficulty of modeling. The absence of periodicity excludes to embody the infinite domain of the material by an individual RVE of finite-size. A solution to this problem is to use

statistically equivalent RVEs (SERVE) [4]. According to this, the real material behavior should be reflected by a series of statistically equivalent RVE-samples instead of a unique one. However, because most existing modeling techniques require considerable manual intervention for the mesh generation, the idea of SERVE has only limited application in the scope of PRMMC materials. Meanwhile, modeling of the real microstructure is much more demanding than the idealized case. Therefore, to author's knowledge, until now the concept of SERVE is confined to idealized microstructure rather than the real one.

The intrinsic randomness of PRMMC materials also restricts material properties to be studied: the accurate prediction of the nonlinear behavior of the composite generally demands larger RVE-size [5]. As consequence and despite their importance, yield strength and ultimate strength of the PRMMC are less frequently investigated than elastic properties. The determination of the global yield condition depends on how the macroscopic plasticity is interpreted, and the contribution in this regards can be traced to Suquet's work [6] who proposed an energetic approach and introduced a definition of the global plastic strain. Basing on this work, the yield strength of several PRMMCs are studied, e.g. 2124 Al-SiC [7] and WC-Co [8].

To obtain the macroscopic ultimate strength of a composite numerically, a two-step approach consisting of limit analysis and homogenization technique can be performed [9]. First, the loading corresponding to the plastic limit is calculated, and then secondly, the obtained result is linked to the overall material behavior through the homogenization technique. The limit analysis within the first step can be carried out either by an incremental method (IM) or a direct method (DM). In contrast to the conventional IM, DM determines the critical loads without taking into account the specific loading history and demands less computational effort [10]. DM are based either on statical theorems [11] or kinematic theorems [12], and results deliver in principle lower and upper bounds of the plastic limit, respectively. Applying DM to evaluate the load bearing capacity of composite materials and to investigate its dependence on the microstructure has been introduced in [13-16] applying the statical approach and in [17-19] applying the kinematical one. However, these studies focus more on the methodology aspect, and the composites taken into consideration are periodic with regular microstructure.

In the present study, we use the DM analogously to the one proposed in [16] and apply it to a typical random PRMMC, WC-Co, to predict its macroscopic ultimate strength as well as the yield strength. These material parameters are calculated also by the IM for comparison. The failure scenario assumed in this study is restricted to the instantaneous collapse of the matrix phase, other mechanisms such as debonding between phases or brittle fracture are neglected. Aware of the randomness of the material, the analysis employs a series of 2D SERVE-models generated from real scanning electron microscope (SEM) images. One focus of the study is to analyze the statistical distribution of a set of global material parameters

2 STATISTICAL STRENGTH PREDICTION THROUGH LIMIT ANALYSIS AND HOMOGENIZATION

2.1 Macroscopic yield strength of an elastic-plastic composite

The homogenization theory links physical fields in two well-separated scales, say the

micro scale $\boldsymbol{y}$ in which structural details of RVE are distinguishable and the macro scale $\boldsymbol{x}$ in which RVE is recognized as a macroscopic point. For a heterogeneous composite, once submitted to an external loading, its microscopic stress field $\boldsymbol{\sigma}$ in $\boldsymbol{y}$ and the macroscopic counterpart to it in $\boldsymbol{x}$ satisfy the relationship:

$$\langle \boldsymbol{\sigma} \rangle = \frac{1}{\Omega}\int_{\Omega} \boldsymbol{\sigma}(y)dv \,. \tag{1}$$

Herein Ω denotes the RVE domain. Angle brackets represent a macroscopic quantity calculated from the volume average. Analogously, the strain in two scales is related as:

$$\langle \boldsymbol{\varepsilon} \rangle = \frac{1}{\Omega}\int_{\Omega} \boldsymbol{\varepsilon}(y)dv \,. \tag{2}$$

When all components of the composite stay in the elastic regime, the relationship between $\langle \boldsymbol{\sigma} \rangle$ and $\langle \boldsymbol{\varepsilon} \rangle$ can be obtained via the effective elasticity tensor $\overline{\boldsymbol{C}}$:

$$\langle \boldsymbol{\sigma} \rangle = \overline{\boldsymbol{C}} : \langle \boldsymbol{\varepsilon} \rangle \,. \tag{3}$$

If anisotropy is negligible, $\overline{\boldsymbol{C}}$ can be characterized by two parameters: the effective Young's modulus $\bar{E}$ and effective Poisson's ratio $\bar{\upsilon}$.

One major characteristic of WC-Co composites is that the irregular microstructure causes severe stress localization. This means the onset of the local plasticity can take place even when $\langle \boldsymbol{\sigma} \rangle$ is fairly low. To describe the contribution of the local plastic deformation in the global scale, Suquet [6] proves that $\langle \boldsymbol{\varepsilon^P} \rangle$ is not a reasonable measure, because it is not the work conjugate pair to $\langle \boldsymbol{\sigma} \rangle$. In contrary, the global plasticity should be measured by the effective plastic strain $\overline{\boldsymbol{\varepsilon}}^{\boldsymbol{P}}$ defined as:

$$\overline{\boldsymbol{\varepsilon}}^{\mathrm{p}} = \langle \boldsymbol{\varepsilon} \rangle - \overline{\boldsymbol{C}}^{-1} : \langle \boldsymbol{\sigma} \rangle \,. \tag{4}$$

According to this definition, the global yield criterion of the material can be defined similarly as that for a metallic material:

$$\langle \boldsymbol{\sigma} \rangle^{Y} = \arg\ \left(\overline{\boldsymbol{\varepsilon}}^{P}_{eq}(\langle \boldsymbol{\sigma} \rangle_{eq}) = 0.2\% \right). \tag{5}$$

Here $\overline{\boldsymbol{\varepsilon}}^{P}_{eq}$ and $\langle \boldsymbol{\sigma} \rangle_{eq}$ indicate the equivalent plastic stain and the equivalent macroscopic stress, respectively, which are defined as:

$$\overline{\boldsymbol{\varepsilon}}^{P}_{eq} = \sqrt{\frac{2}{3}(\overline{\boldsymbol{\varepsilon}}^{P})' : (\overline{\boldsymbol{\varepsilon}}^{P})'} \,, \tag{6}$$

$$\langle \boldsymbol{\sigma} \rangle_{eq} = \sqrt{\frac{3}{2}\langle \boldsymbol{\sigma} \rangle' : \langle \boldsymbol{\sigma} \rangle'} \,, \tag{7}$$

Here, the apostrophe indicates the deviatoric part of the tensors. It is worthy to note that, although macroscopically WC-Co are elastically and plastically isotropic, this is not true for specific RVEs. Therefore, the average of the global strength in two orthogonal directions should be taken as the material strength.

2.2 Limit analysis based on the incremental and the direct method

The aim of limit analysis is to identify the macroscopic admissible load domain $\mathcal{L}$ defined as:

$$\mathcal{L} = \left\{ \langle \boldsymbol{\sigma} \rangle : f(\boldsymbol{\sigma}(y), \sigma^Y(y)) \le 0, \forall y \in \Omega \right\}, \tag{8}$$

where f stands for the yield function, σ^Y denotes the local yield strength. In this paper we use the von Mises yield function without hardening:

$$f(\boldsymbol{\sigma}(y), \sigma^Y(y)) = \sqrt{\frac{3}{2}\boldsymbol{\sigma}'(y) : \boldsymbol{\sigma}'(y)} - \sigma^Y(y) . \tag{9}$$

Since hardening is neglectedr, σ^Y is time-independent for every material point.

Limit analysis can be carried out by IM or DM; in current study both approaches are investigated. To determine numerically the macroscopic ultimate strength $\langle \sigma \rangle^U$ through IM, a macroscopic stress $\langle \boldsymbol{\sigma} \rangle$ is applied incrementally to a RVE model. For each increment, the finite element (FE) program calculates the change of global strain and updates $\langle \boldsymbol{\varepsilon} \rangle$ accordingly. Once the applied loading has reached a critical level, the program terminates due to the non-convergence and the eventual stress is recognized as the limit one which corresponds to a point lying on the boundary of $\mathcal{L}$ [20].

The DM applied in this study is based on the static shakedown theorem by Melan [21]. Considering a RVE having elastic-plastic deformation, the total stress field can be decomposed into two parts: $\boldsymbol{\sigma}^E$ representing the fictitious elastic stress when the same loading is applied on the purely elastic reference RVE and $\boldsymbol{\rho}$ represents residual stress field which remains after removal of external loadings:

$$\boldsymbol{\sigma}(y,t) = \boldsymbol{\sigma}^E(y,t) + \boldsymbol{\rho}(y,t) . \tag{10}$$

The residual stress field is a self-equilibrium field, thus it satisfies:

$$\nabla \cdot \boldsymbol{\rho}(y,t) = \mathbf{0}, \quad \forall y \in \Omega , \tag{11}$$

$$\boldsymbol{\rho}(y,t) \cdot \boldsymbol{n} = \mathbf{0}, \quad \forall y \in \partial\Omega_T . \tag{12}$$

Here, $\partial\Omega_T$ denotes the boundary of a RVE with prescribed stresses and $\boldsymbol{n}$ the outer normal.

According to the applied theorem, a set of NL monotonic loads $\{\boldsymbol{P_i}\}$ does not exceed the load bearing capacity of the material by means of plastic limit if, and only if, a positive load factor $\alpha > 1$ and a time-independent residual stress field $\overline{\boldsymbol{\rho}}$ can be found, whose superposition with $\boldsymbol{\sigma}^E$ entailed from $\{\boldsymbol{P_i}\}$ complies with the yield condition at any given point $\boldsymbol{y}$. In the light of this statement, the load set leading to the plastic limit can be characterized by a maximal loading factor α where:

$$\alpha^{LM} = \max . \ \alpha \tag{13}$$

$$s.t. \ \ f\left(\alpha \boldsymbol{\sigma}^E \left(\sum_{i=1}^{NL} P_i(y) \right) + \overline{\boldsymbol{\rho}}(y), \sigma^Y(y)\right) \le 0, \quad \forall y \in \Omega .$$

By comparing (13) to (8), one can notice that DM is capable of determine the same domain $\mathcal{L}$ if referring $\{\boldsymbol{P_i}\}$ to $\langle \boldsymbol{\sigma} \rangle$. Meanwhile, due to the linearity of the elastic stress:

$$\boldsymbol{\sigma}^{E}\left(\sum_{i=1}^{NL}\boldsymbol{P}_{i}(y)\right)=\sum_{i=1}^{NL}\boldsymbol{\sigma}^{E}\left(\boldsymbol{P}_{i}(y)\right), \tag{14}$$

$\boldsymbol{\sigma}^{E}$ can be acquired also through the summation defined in (14).

The numerical solution of α^{LM} involves a descretization of the original problem (13) in the context of FE method and solving a nonlinear programming problem. For the 2D-plane strain case, the discretization of (13) yields:

$$(\mathcal{P}_{ORI})\ \alpha^{LM}=\max_{\bar{\rho}}\ \alpha \tag{15}$$

$$[\boldsymbol{C}]\{\bar{\boldsymbol{\rho}}\}=0,\ \text{ where } [\boldsymbol{C}]\in R^{(2NK-LC)\times 3NGS},$$

$$f(\alpha\boldsymbol{\sigma}_{i}^{\boldsymbol{E}}+\bar{\boldsymbol{\rho}}_{i},\sigma_{i}^{Y})\le 0, i\in[1,NGS].$$

Here *NK* represents the total number of nodes, *NGS* the total number of Gaussian points, *LC* the number of constrained degree of freedom, $[\boldsymbol{C}]$ the equilibrium matrix with dimension $(2NK\text{-}LC)\times 3NGS$.

To improve the computational efficiency, (15) is mathematically reformulated according to [22] into a more capable form where convex quadratic inequality constraints are replaced by the Euclidean ball constraints:

$$(\mathcal{P}_{Reform})\ \alpha^{LM}=\max\ \alpha \tag{16}$$

$$\sum_{r=1}^{NG}\boldsymbol{A}_{r}u_{r}+\boldsymbol{B}\boldsymbol{x}-\alpha w=0,\ \text{ where } [\boldsymbol{A}_{r}]\in R^{(2NK-LC)\times 3},[\boldsymbol{B}]\in R^{(2NK-LC)\times NG},u_{r}\in R^{3},x\in R^{NG},w\in R^{2NK},$$

$$\left\|u_{r}\right\|\le 1,\ \text{ for } r=1..NGS.$$

To handle the large-scaled non-linear programming problem (16), the optimization solver IPOPT [23] based on the interior-point method [24] is applied.

Similar as the yield strength, the ultimate strengths of the RVEs in different directions are in general not uniform. To reduce the global anisotropy's impact on the objectivity of the prediction, a more sophisticated method rather than calculating the average was applied. This method has been successfully utilized to predict the limit strength of a fiber-reinforced composite [16]. A major benefit of this method is that not only the strength in two orthogonal directions, but also the stress multi-axiality is considered. The ultimate strength is calculated for several combinations of two in-plane normal stresses, i.e. $\langle\boldsymbol{\sigma}\rangle_{11}$ and $\langle\boldsymbol{\sigma}\rangle_{22}$. Afterwards, the acquired results are projected to the π-plane and $\langle\sigma\rangle^{Y}$ is obtained by fitting the projected domains to the von Mises criterion by means of the least square method.

2.3 Statistical evaluation of the global material strength

The WC-Co composite is a typical random material. To interpret the impact of randomness, a statistical study is carried out. For this, we employed few simple statistical measures including mean value μ; standard deviation *SD* and the coefficient of variation C_{μ}:

$$C_{\mu}=\frac{SD}{\mu}. \tag{17}$$

Since C_μ excluded the influence of the absolute magnitude of an investigated object, it is an appropriate measure to compare the degree of disparity between different objects.

To perform the statistical analysis, we used 30µm-by-30µm finite element RVE models. All these models are based on real WC-Co microstructures gained from a scanning electron microscope (SEM) observation using a backscattering detector [25]. All samples belong to a WC-30Co hard metal, meaning that the cobalt content constitutes the 30% weight and average carbide grain size is $d_{WC} = 2.35\mu m$. During the sample preparation, metallographic specimens were ground, polished and etched with Murakami solution in order to differentiate between neighboring WC-grains. As seen in Figure 1, the dark grey areas are Co, while the bright areas are the WC grains with their characteristic prismatic shape. To convert a SEM image to its corresponding FE model, we employed an automatic technique developed in [26]. This technique is capable of generating a triangular element based adaptive finite element mesh. It adopts a denser mesh close to phase interfaces and a coarser mesh elsewhere. The resulting mesh generated from this technique appears similarly to Figure 1.

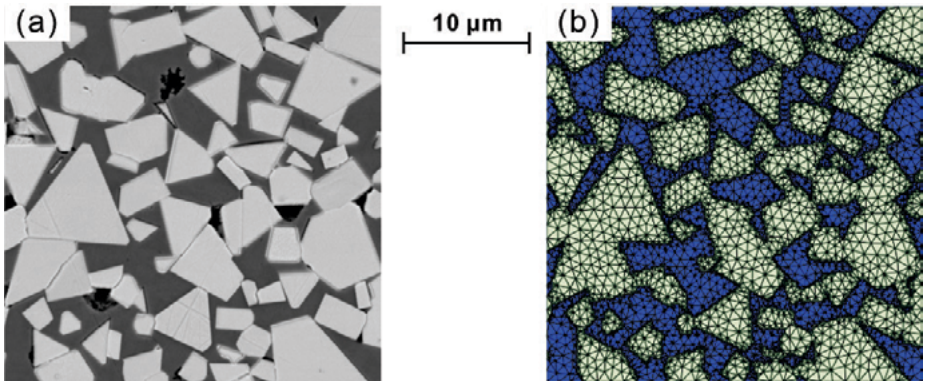

Figure 1: SEM image and finite element RVE model of the WC-Co

3 NUMERICAL EXAMPLES

3.1 Details of the Finite element model

Our numerical study is based on a model group consisting of 10 RVE samples generated from the automatic technique explained above and encoded consecutively from 1 to 10. Each of these samples has a unique microstructure and for all of them we use first order triangular plane strain elements, because this element type is proven to capture the global behavior of the WC-Co composite better than e.g. the plane stress element [8]. Within each model, elements covering the non-critical regions were assigned a global size of 0.8µm whereas the ones lying on the phase boundaries were assigned with an edge length of 0.2µm. For this configuration, the number of elements varies between 6000-9000. The material properties for both phases are described in Table 1. We restricted our investigation to the case of geometrical linearity.

The commercial FE solver ABAQUS is used for both IM and DM. To apply the global loading, we introduce for each edge a reference point and link it to the nodes lying on the edge. This way, a concentrated force corresponding to $\langle \boldsymbol{\sigma} \rangle$ can be applied on the reference point. Since by this procedure the DoF of nodes are all equal to the coupled reference point,

all edges remain straight during the deformation process.

Table 1: material properties

	E [GPa]	υ [−]	σ^Y [MPa]
WC	700	0.24	2000
Co	210	0.30	279

As mentioned, DM determines directly the ultimate strength in two steps: first, the purely elastic reference RVE is loaded alternately with arbitrarily chosen global stress $\langle\boldsymbol{\sigma}\rangle_{11}$ and $\langle\boldsymbol{\sigma}\rangle_{22}$ and the according microscopic stress fields $\boldsymbol{\sigma}_{11}^E$ and $\boldsymbol{\sigma}_{22}^E$ are calculated. After that, as shown in Figure 2, the resulting stress fields are scaled by $p_1 = \cos\alpha$ and $p_2 = \sin\alpha$ respectively and then superposed to represent the stress field under multi-axial global load $\langle\boldsymbol{\sigma}\rangle^{\mathrm{E}}$. In this manner, by iterating the value of α inside interval $[0, \pi]$, a series of load vectors representing different load combinations can be obtained. For each load vector, the associated mathematical programming problem (16) is solved. The obtained macroscopic domains for all these predefined load vectors are fitted to a global von-Mises criterion to calculate $\langle\sigma\rangle^U$.

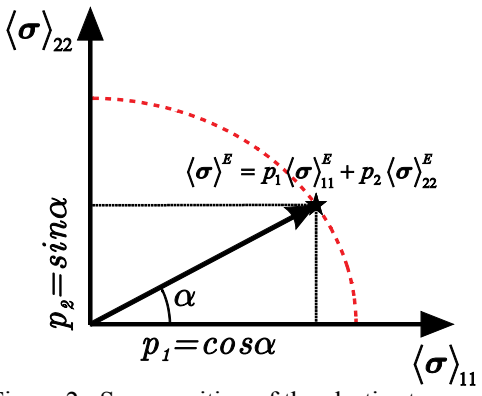

Figure 2: Superposition of the elastic stress

Besides DM, we also applied the conventional IM to determine $\langle\sigma\rangle^Y$ and $\langle\sigma\rangle^U$ on the same group of RVE models. In these calculations, $\langle\boldsymbol{\sigma}\rangle_{11}$ and $\langle\boldsymbol{\sigma}\rangle_{22}$ are set uniformly to 2000 MPa, which is the strength of the reinforcement phase. To calculate $\langle\sigma\rangle^Y$, two given loadings are prescribed individually and a python based script is developed to evaluate in each increment the $\bar{\varepsilon}_{ep}^P$ defined in (4). Once this value attains 0.2%, the associated $\langle\boldsymbol{\sigma}\rangle$ is identified as the yield strength. For the determination of $\langle\sigma\rangle^U$, a similar process as in DM is followed. During the implementation, $\langle\boldsymbol{\sigma}\rangle_{11}$ and $\langle\boldsymbol{\sigma}\rangle_{22}$ are combined by a predefined angle α and applied to each RVE jointly. In this case, $\langle\sigma\rangle^U$ refers to the load magnitude where the calculation stops to converge.

3.2 Results of numerical studies and statistical analysis

The plastic limit domain calculated by DM is demonstrated in Figure 3. On the left side, the domain for each RVE is shown and on the right the two extreme cases and the average of all RVE-models. As expected, the individual plastic limit domains are scattered. It can be noted from the figure that anisotropy for all models is small, with values $\langle\boldsymbol{\sigma}\rangle_{11}^U$ and $\langle\boldsymbol{\sigma}\rangle_{22}^U$ rather

close to each other. For values of α near 45°, the strength becomes quite large, because $\alpha = 45°$ corresponds to the case$\langle\boldsymbol{\sigma}\rangle_{11} = \langle\boldsymbol{\sigma}\rangle_{22}$; for all existing models this condition indicates a globally hydrostatic stress. Since the hydrostatic part does not contribute to the von-Mises yield condition, material at this point can sustain high global stress. When the load domain shown in Figure 3(R) is projected to the π-plane, it becomes an imperfect semi-circle as depicted in Figure 4. By fitting this curve to the von-Mises yield criterion, which constitutes a perfect ball in this space, a direction-independent $\langle\sigma\rangle^U$ can be obtained.

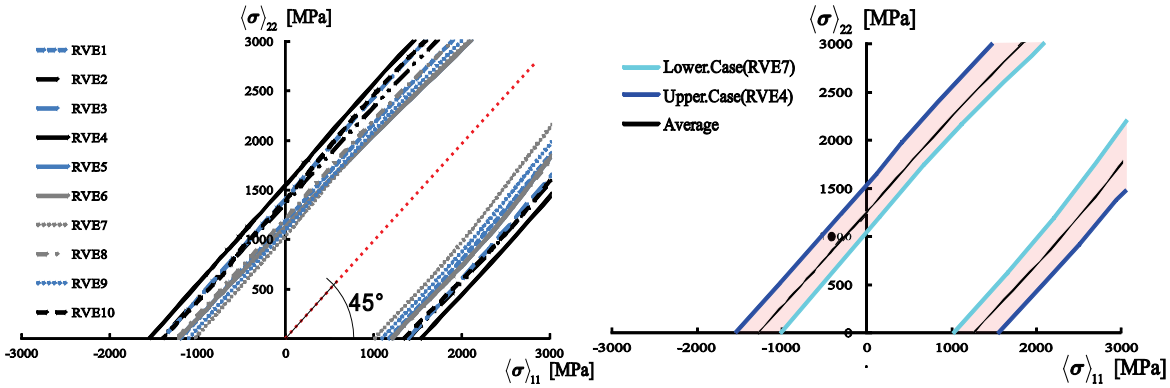

Figure 3: Domain of the plastic limit obtained by DM for: (L) each RVE model (R) Average and two extreme cases

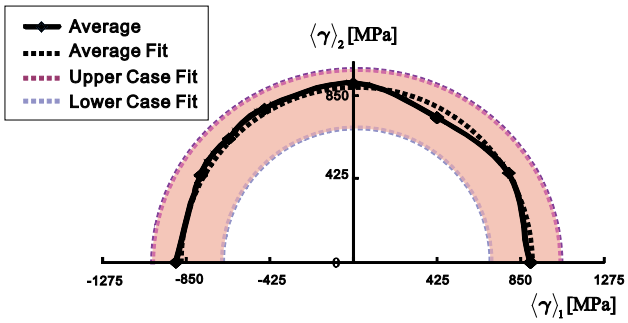

Figure 4: Projection of plastic limit domain in the π-plane

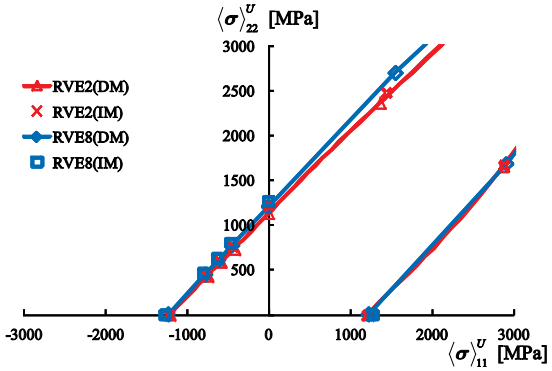

Figure 5: Comparison between plastic limit domains for selected RVEs

For a concise presentation of the results, we do not show the plastic limit domains for each RVE obtained by IM since they are almost same to those obtained by DM. Instead, we

selected two RVE-models arbitrarily and compared their plastic limit domains calculated by the two approaches (Figure 5). It can be observed that in general strength calculated by IM is slightly lower than that by DM. We suppose that this is caused by the minimum incremental step size in ABAQUS. Smaller step length would postpone the point of non-convergence.

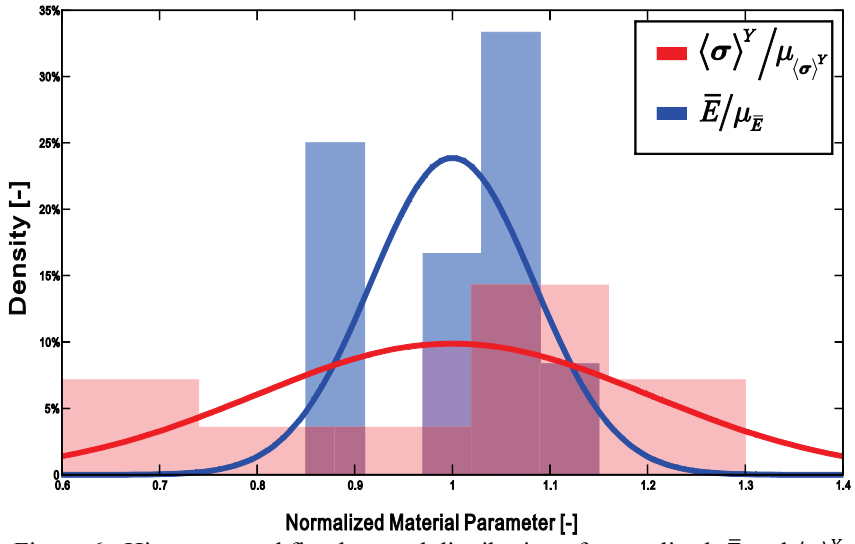

Figure 6: Histogram and fitted normal distribution of normalised $\bar{E}$ and $\langle\sigma\rangle^Y$

Table 2: Statistics of several critical global material properties

	μ	SD	C_μ
$\bar{E}$ [GPa]	396.7	33.5	0.084
$\bar{\upsilon}$ [-]	0.264	0.004	0.018
$\langle\sigma\rangle^Y$[MPa]	636.9	144.7	0.227
$\langle\sigma\rangle^U$[MPa]	1054.3	137.9	0.131

Limit analysis has revealed that the global strength obtained by RVE-models of same size and constituents may vary significantly due to the different morphology. A similar disparity can be observed also from the histograms in Figure 6. In this figure, both given parameters, $\bar{E}$ and $\langle\sigma\rangle^Y$, are scaled to their average value to enable a transverse comparison. By comparing these normalized parameters, it is obvious that the scatters for different global parameters are as well significant. To quantify the disparity of a distribution more precisely, we perform statistical analysis and characterize the distribution by the three previously introduced parameters μ, SD and C_μ. The results are shown in Table 2. One can see that the C_μ of global elastic properties described by $\bar{E}$ and $\bar{\upsilon}$, are lower than those related to plasticity, $\langle\sigma\rangle^Y$ and $\langle\sigma\rangle^U$. Because all models are same in size and constituents, the magnitude of C_μ actually reflects the impact of morphology and the significance of the local material behavior. We conclude that the morphology critically influences the global yield point. As a consequence, in order to accurately predict$\langle\sigma\rangle^Y$, either larger RVE size or more RVE samples have to be employed.

4 DISCUSSION AND CONCLUSION

It is shown in this paper how to incorporate limit analysis and homogenization theory to predict the global strength of the PRMMC material. The study focuses on the implementation of limit analysis through the direct method in extension to studies devoted to periodic composites. We overcame in this study the obstacle to determine RVE for such material. In additional, the RVEs investigated here contain normally 6000 to 9000 elements which lead to large scale optimization problems. By using interior-point method and reforming the original problem to the form proposed in [22], the problems are solved efficiently. Based on the statistical investigation of 10 RVE models converted from SEM images, several major conclusions can be summarized as follows:

i. The plastic limit predicted by the direct method is almost identical to that calculated by the conventional incremental method. It convinced that, the direct method can successfully handle a problem of current scale and level of complexity.
ii. On the one hand, by means of all selected global measures including global elasticity and strength, all RVEs illustrate negligible anisotropy. But on the other hand, the disparity among them is still remarkable. This phenomenon reveals that isotropy should be taken as a necessary but insufficient criterion in validating the representativeness of an individual RVE.
iii. Among all picked global material features, the distribution of global yield strength has the largest scatter. This phenomenon indicates that this material feature has the strongest dependence on the micro-structural morphology, i.e., it is very sensitive to the local behavior of the composite.

At last, the authors would like to emphasize that the failure scenario assumed in this paper is restrictive; some material behaviors such as damage and plastic hardening are not accounted for, since they result more complicated mathematical programming problem. Nevertheless, these effects would be studied in our future works.

REFERENCES

[1] Ibrahim, I.A., Mohamed, F.A., and Lavernia, E.J., Particulate reinforced metal matrix composites – a review. *J. Mater. Sci.* (1991) **26**:1137-1156.
[2] Torquato, S., *Random Heterogeneous Materials: Microstructure and Macroscopic Properties*, Springer, (2002).
[3] Chawla, N., and Chawla, K.K., Microstructure-based modeling of the deformation behavior of particle reinforced metal matrix composites. *J. Mater. Sci.* (2006) **41**:913-925.
[4] Swaminathan, S., Ghosh, S., and Pagano, N.J., Statistically equivalent representative volume elements for unidirectional composite microstructures: Part I - Without damage. *J. Compos. Mater.* (2006) **40**:583-604.
[5] Galli, M., Cugnoni, J., and Botsis, J., Numerical and statistical estimates of the representative volume element of elastoplastic random composites. *Eur. J. Mech. A-solid.* (2012) **33**:31-38.
[6] Suquet, P.M., "Elements of homogenization for inelastic solid mechanics " *Homogenization techniques for composite media : lectures delivered at the CISM International Center for Mechanical Sciences, Udine, Italy, July 1-5, 1985*, 272, E. Sanchez-Palencia, A. Zaoui and International Centre for Mechanical Sciences., eds., pp. 194-278, Berlin ; New York: Springer-Verlag, 1987.

[7] Galli, M., Botsis, J., and Janczak-Rusch, J., An elastoplastic three-dimensional homogenization model for particle reinforced composites. *Comp. Mater. Sci.* (2008) **41**:312-321.
[8] Sadowski, T., and Nowicki, T., Numerical investigation of local mechanical properties of WC/Co composite. *Comp. Mater. Sci.* (2008) **43**:235-241.
[9] Weichert, D., Hachemi, A., and Schwabe, F., Application of shakedown analysis to the plastic design of composites. *Arch. Appl. Mech.* (1999) **69**:623-633.
[10] Weichert, D., and Ponter, A., *Limit states of materials and structures - Direct methods*, Dordrecht u.a., Springer Netherland, (2009).
[11] Hill, R., A Variational Principle of Maximum Plastic Work in Classical Plasticity. *Q. J. Mech. Appl. Math.* (1948) **1**:18-28.
[12] Drucker, D.C., Limit analysis of two and three dimensional soil mechanics problems. *J. Mech. Phys. Solids.* (1953) **1**:217-226.
[13] Magoariec, H., Bourgeois, S., and Débordes, O., Elastic plastic shakedown of 3D periodic heterogeneous media: a direct numerical approach. *Int. J. Plasticity.* (2004) **20**:1655-1675.
[14] Hachemi, A., Mouhtamid, S., and Weichert, D., Progress in shakedown analysis with applications to composites. *Arch. Appl. Mech.* (2005) **74**:762-772.
[15] Zhang, H.T., Liu, Y.H., and Xu, B.Y., Plastic Limit Analysis of Ductile Composite Structures from Micro- to Macro-Mechanical Analysis. *Acta Mech. Solida. Sin* (2009) **22**:73-84.
[16] Chen, M., Hachemi, A., and Weichert, D., "Shakedown and Optimization Analysis of Periodic Composites," *Limit State of Materials and Structures*, pp. 45-69: Springer, 2013.
[17] Li, H.X., Liu, Y.H., Feng, X.Q., and Cen, Z.Z., Micro/macromechanical plastic limit analyses of composite materials and structures. *Acta Mech. Solida. Sin* (2001) **14**:323-333.
[18] Maier, G., On some issues in shakedown analysis. *J. Appl. Mech-t. Asme.* (2001) **68**:799-807.
[19] Li, H.X., Microscopic limit analysis of cohesive-frictional composites with non-associated plastic flow. *Eur. J. Mech. A-solid.* (2013) **37**:281-293.
[20] Schwabe, F., *Ph.D. Dissertation: Einspieluntersuchungen von Verbundwerkstoffen mit periodischer Mikrostruktur*, IAM, RWTH Aachen, (2000).
[21] Melan, E., Zur Plastizität des räumlichen Kontinuums. *Ingenieur-Archiv* (1938) **9**:116-126.
[22] Akoa, F., Hachemi, A., Le, T.H.A., Mouhtamid, S., and Pham, D.T., Application of lower bound direct method to engineering structures. *J. Global. Optim.* (2007) **37**:609-630.
[23] Wächter, A., and Biegler, L.T., On the implementation of an interior-point filter line-search algorithm for large-scale nonlinear programming. *Math. Program.* (2006) **106**:25-57.
[24] ElBakry, A.S., Tapia, R.A., Tsuchiya, T., and Zhang, Y., On the formulation and theory of the Newton interior-point method for nonlinear programming. *J. Optimiz. Theory. App* (1996) **89**:507-541.
[25] Keusemann, S., Broeckmann, C., and Magin, M., Fatigue Crack Propagation in WC-Co Hardmetals. *Proceeding of EURO PM Powder Metallurgy Congress & Exhibitions* (2011) **1**.
[26] Chen, G., Ozden, U.A., Bezold, A., and Broeckmann, C., A statistics based numerical investigation on the prediction of elasto-plastic behavior of WC–Co hard metal. *Comp. Mater. Sci.* (In Press).